



This is an author produced version of a paper published in
Journal of Materials Chemistry B.

This paper has been peer-reviewed but may not include the final publisher
proof-corrections or pagination.

Citation for the published paper:

O.L. Galkina, V.K. Ivanov, A.V. Agafonov, G.A. Seisenbaeva, V.G.

Kessler. (2015) Cellulose nanofiber–titania nanocomposites as potential drug
delivery systems for dermal applications. *Journal of Materials Chemistry B*

Volume: 3, pp 1688-1698.

<http://dx.doi.org/10.1039/C4TB01823K>.

Access to the published version may require journal subscription.

Published with permission from: Royal Society of Chemistry.

Standard set statement from the publisher:

Epsilon Open Archive <http://epsilon.slu.se>

Cellulose nanofibers – titania nanocomposites as potential drug delivery systems for dermal applications

O.L. Galkina^{ab}, V.K. Ivanov^{c,d}, A.V. Agafonov^a, G.A. Seisenbaeva^{b,e}, and V.G. Kessler^{b,e*}

^aInstitute of Solution Chemistry of the Russian Academy of Sciences, Akademicheskaya St.,1, Ivanovo, Russia, e-mails: olga.galkina@slu.se, ava@isc-ras.ru;

^bDepartment of Chemistry and Biotechnology, Swedish University of Agricultural Sciences, 750 07 Uppsala, Sweden, e-mails: gulaim.seisenbaeva@slu.se, vadim.kessler@slu.se

^cKurnakov Institute of General and Inorganic Chemistry, Leninskii prosp. 31, Moscow, Russia, e-mail: van@igic.ras.ru

^dNational Research Tomsk State University, 36 Lenin Av., Tomsk, 634050, Russia,

^eCaptiGel AB, Virdings allé 32B, 75450 Uppsala, Sweden.

In this work, new efficient drug delivery systems based on cellulose nanofibers – titania nanocomposites grafted with three different types of model drugs such as Diclofenac sodium, Penicillamine-D and Phosphomycin were successfully synthesized and displayed distinctly different controlled long-term release profiles. Three different methods of medicine introduction were used to show that various interactions between TiO₂ and drug molecule could be used to control the kinetics of long-term drug release. All synthesis reactions were carried out in aqueous media. Morphology, chemical structure and properties of the obtained materials were characterized by SEM, TEM and AFM microscopy, Nanoparticle Tracking analysis, X-ray diffraction, and TGA analysis. According to FT-IR and UV-Vis spectroscopy data, the titania binds to cellulose nanofibers via formation of ester bonds and to drug molecules via formation of surface complexes. The drug release kinetics was studied in vitro for Diclofenac sodium and Penicillamine-D spectrophotometrically and for Phosphomycin using a radio-labeling analysis with ³³P-marked ATP as a model phosphate-anchored biomolecule. The results demonstrated that the obtained nanocomposites could potentially be applied in transdermal drug delivery for anesthetics, analgesics and antibiotics.

Introduction

Nanocomposites based on nanocellulose, nano- or microfibrillar cellulose, cellulose nanofibers are new generation nanomaterials possessing wide range of practical applications in such domains as pharmacology¹ and medicine², tissue engineering³⁻⁵, biosensors⁶, microfluidics elements⁷, materials for microencapsulation⁸ and drug delivery⁹⁻¹², as permselective membranes¹³, and as a barrier to protect mucosal tissues^{14,15}. The nanoscale cellulose possesses a whole complex of unique properties typical for nanomaterials in general, such as high specific surface area, enhanced chemical reactivity, high mechanical durability, together with biocompatibility, biodegradability, and non-toxicity, which make it an excellent candidate for drug release applications.

Due to these specific properties, bandage materials, transdermal patches, tablet binder, disintegrated vehicle for peptide and gene delivery can be obtained based on nanoscale cellulose, and raw materials for their production are almost unlimited¹⁶⁻¹⁸. In particular, nanocrystalline cellulose has been used as a matrix-former material for long-lasting sustained drug delivery and for food packing materials¹⁹⁻²².

In recent years, the application of inorganic materials for bioencapsulation and controlled drug release has attracted considerable attention^{23,24}. Particularly, nanosized titania, due to its unique photophysical and chemical properties, non-toxicity, and high biocompatibility, is a promising material and has great prospects for practical application in these fields. Generally, nanoporous titania is used as drug nanocarriers^{25,26}. In a recent study, Li et al.²⁷ reported a novel drug controlled release system based on hybrid phosphonate-TiO₂ mesoporous nanoparticles as a scaffold, which was loaded with suitable drug molecules.

To the best of our knowledge, no attempts have been made in combining the advantageous characteristics of nanocrystalline cellulose with the specific properties of nanosized titania by modification. This approach, however, has potential to open endless possibilities for creation of new efficient drug delivery systems with a whole range of functional properties. Previously, we obtained TiO₂/cotton composites with high photocatalytic and antibacterial activity^{28,29}. The aim of the present work was to develop potential application of the nanocomposites based on cellulose nanofibers and grafted titania as drug delivery system.

Experimental

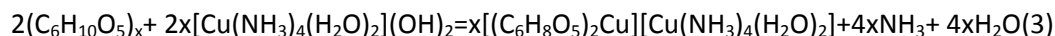
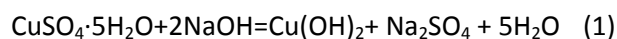
Copper sulfate (CuSO₄·5H₂O), sodium hydroxide (NaOH), ammonia (NH₄OH, 25 wt%), sulfuric acid (H₂SO₄, 98 wt%), 1,2,3,4 – butanetetracarboxylic acid (BTCA), sodium hypophosphite (NaH₂PO₂), Diclofenac sodium salt (C₁₄H₁₀Cl₂NNaO₂, Mw ~318.13), Penicillamine D ((CH₃)₂C(SH)CH(NH₂)CO₂H, Mw~149.21) Phosphomycin disodium salt (C₃H₅Na₂O₄P, Mw~182.02), polyvinyl alcohol (PVA, Mw 146,000-186,000) were purchased from Sigma-Aldrich. The TiO₂ nanosol was produced by CaptiGel AB, Uppsala, Sweden. Raw cotton (100%) was used as a starting material.

Synthetic procedures

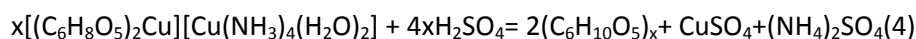
Preparation of cellulose nanofibers

For obtaining cellulose nanofibers we have developed a method based on the use of copper ammonium complex for converting raw cotton (RC) into a molecular solution with subsequent regeneration by means of acid hydrolysis.

5 g of copper (II) sulfate were dissolved in 100 ml of distilled water, and then sodium hydroxide (5M) was added until precipitation (eq.1). The copper hydroxide precipitate was thoroughly washed by distilled water to remove Na⁺. Then, the precipitate was dissolved in 200 ml of ammonia (25 wt%) giving a deep blue solution of tetraamminediaquacopper dihydroxide (Schweitzer's reagent) (eq.2). Two grams of raw cotton were added to the cuprammonium solution. When cotton was completely dissolved in the Schweitzer's reagent (eq. 3), the solution was further used for obtaining aqueous suspension of cellulose nanofibers.



For this purpose, 25 ml of Schweitzer's reagent solution, containing the dissolved cotton, was added into 140 ml of the sulfuric acid solution (40 wt%) and stirred vigorously at 60 °C for 4 hours. After that, hydrolysis was immediately quenched by adding 500 ml of cold distilled water to the reaction mixture. The sulfuric acid was removed from the resulting suspension by centrifuging with distilled water until pH=6.



Preparation of nanocomposites loaded with different drugs

Firstly, to cross-link titania nanoparticles with cellulose nanofibers, 1,2,3,4-butane-tetracarboxylic acid was used as a spacer in the presence of sodium hypophosphite (SHP). For this, the obtained aqueous suspensions of cellulose nanofibers were treated by BTCA (0,002 mol) with SHP (0,002 mol) aqueous

solution at 70°C during 2 h. Next, titania nanosol was added to the obtained solution and the modification was carried out at 70°C during 2 h. The obtained nanocomposites were dried at 40°C for 48 h.

Introduction of drugs

The BTCA-treated cellulose nanofibers were modified by TiO₂ nanosol and drug by using three different methods.

Method #1 (M1): drug powder (Diclofenac sodium salt - DS, Penicillamine D - PCA-D or Phosphomycin disodium salt - Phos) was initially dissolved in titania nanosol and thereafter the obtained solution was added to an aqueous suspension of cellulose nanofibers and kept at 70°C during 2 h. The obtained nanocomposites were dried at 40°C for 48 h.

Method #2 (M2): The drug powder (DS, PCA-D or Phos) was initially dissolved in water and then added together with the titania nanosol simultaneously to an aqueous suspension of cellulose nanofibers. The mixture was kept at 70 °C during 2 h. The obtained nanocomposites were dried at 40°C for 48 h.

Method #3 (M3): firstly, TiO₂ nanosol was added to an aqueous suspension of cellulose nanofibers and kept at 70°C during 2 h. Then, an already dissolved drug powder (DS, PCA-D or Phos) in water was added to the solution and kept at 70 °C during 2 h. The obtained nanocomposites were dried at 40°C for 48 h. The composition of the obtained samples and the method of drug modification are presented in the Table 1. In order to obtain nanocomposites as a film, 3% of PVA was used.

Structure characterization

Scanning and transmission electron microscopy images of the samples were obtained using Carl Zeiss NVision. The elemental analysis of pure cellulose nanofibers and nanocomposites was carried out by a HITACHI TM-1000 scanning electron microscope equipped with an EDX detector. For analysis a drop of each of the diluted suspensions was deposited in the holder with a carbon pad and allowed to dry.

Atomic force microscope (AFM) studies were carried out using a Bruker MultiMode 8 microscope. Pure cellulose nanofibers (PCNF) and nanocomposite based on cellulose nanofibers modified with TiO₂ (CNF_TiO₂) were applied on carbon pad having clean surface.

For the aqueous suspensions of PCNF and CNF_TiO₂ samples, nanoparticle tracking analysis measurements based on Brownian motion of nanoparticles were carried out using a NanoSight instrument, permitting to determine the hydrodynamic size and particle size distribution in real time.

IR spectra of all samples were obtained with a Perkin Elmer FT-IR spectrometer Spectrum-100. A total of 8 scans were carried out on wavenumbers from 400 cm⁻¹ to 4000 cm⁻¹, in transmittance mode. All spectra were smoothed and baseline corrected.

Thermo-gravimetric analysis was carried out in air at a heating rate of 10 °C/min, using a Perkin-Elmer TGA-7 or Pyris 1 device.

The X-ray powder diffraction (XRD) studies were carried out at room temperature using a Bruker APEX II CCD diffractometer (Mo K α 0,71, graphite-monochromator). The main diffraction peak was integrated and used to calculate the crystalline index (CrI,%) of the samples:

$$\text{CrI}(\%) = (\text{I}_{\text{total}} - \text{I}_{\text{am}}) / \text{I}_{\text{total}} \times 100$$

where I_{total} is the scattered intensity at the main peak of cellulose I or II, and I_{am} is the scattered intensity due to the amorphous portion evaluated as the minimum intensity between the main and secondary peaks.

Radiological studies of model drug adsorption

The measurements of uptake and release from pure cellulose nanofibers and nanocomposite based on titania and cellulose nanofibers were performed by Ridgeview Instrument AB, exploiting Ligand Tracer™ White technology, using ³³P-labeled (ATP) (adenosine 5"-triphosphate, substitution on γ -phosphorus atom, 1 ml of solution with 1mCurie total β -activity) as model compound^{30,31}. A part of sample was deposited on a PMMA Petri dish as dispersion in toluene and immobilized by drying in air. Association solution (3.33 ml

of MQ with 0.1% Tween 20) was added to the dish that was mounted in an inclined position into the instrument and subjected to rotation so that the immobilized material was periodically wet by solution and its β -emission was registered immediately afterwards. 1 μ l of ^{33}P -marked ATP solution (resulting in 1nM of ^{33}P -ATP in the dish) was added after 40 min and one more portion of 2 μ l of ^{33}P -marked ATP solution of ^{33}P -marked ATP solution (resulting in ~ 3 nM of ^{33}P -ATP in the dish) – after 23 hours, corresponding to the start of saturation in the observed adsorption. When the adsorption equilibrium was achieved (after 43 hours), the mother liquor was replaced by the dissociation solution (phosphate buffer solution (pH 7.4) with 0.1% Tween 20), and the decrease in radioactivity in the material was followed in the same way.

***In vitro* drug release**

The *in vitro* release studies of Diclofenac Sodium were carried out by placing the nanocomposites containing TiO_2 and DS in definite volume (300 ml) of releasing medium (10-fold isotonic NaCl solution) at constant temperature ($37\pm 0.5^\circ\text{C}$) on constant stirring at 100 rpm³². To investigate the release profile of Penicillamine D, the nanocomposites containing TiO_2 and PCA-D were incubated in 300 ml of citrate buffer at constant temperature ($37\pm 0.5^\circ\text{C}$) on constant stirring at 100 rpm³³. At determined time intervals, 1 mL of each solution was taken out for analysis, and the same volume of fresh medium was added to maintain a constant volume. Diclofenac and Penicillamine D content in each aliquot was determined by spectrophotometry. All the experiments were made three times to get an indication about the reproducibility. UV–Vis quantitative analysis of drugs was performed on a UV/Vis spectrophotometer UV-1800. A linear calibration curve for DS and PCA-D was obtained at 278 nm and 270 nm, respectively. Released drug was determined by using the following equation:

$$\text{Drug release (\%)} = (\text{released drug})/(\text{total drug})\times 100$$

where released drug was calculated from the drug concentration measured in the total volume and total drug was the amount loaded in the obtained sample.

Results and discussion

I. Characterization of pure cellulose nanofibers and the nanocomposite based on cellulose nanofibers modified with TiO_2

The surface morphology and size distribution of pure cellulose nanofibers and obtained nanocomposites based on cellulose nanofibers and titania were analyzed by atomic force microscopy, transmission and scanning electronic microscopes together with detailed EDX analysis of representative samples. Fig.1 (a,b) displays the SEM images of the PCNF sample surface. It could be noted (see Fig.1(a)) that the surface of pure cellulose nanofibers exhibited smooth, homogeneous structures and didn't contain any contaminations, as confirmed by the EDX. Figure 1 shows also the TEM images of PCNF (b) and CNF_ TiO_2 (d). Pure cellulose nanofibers have a rod shape, and their rough average length and diameter were about 15 and 5 nm, respectively. The surface morphology for CNF_ TiO_2 sample is considerably different from that of pure cellulose nanofibers (Fig.1c,d). After TiO_2 modification, the CNF_ TiO_2 sample has uniform morphology and contains TiO_2 nanoparticles evenly distributed over the whole surface. Fig 1(d) also shows quantitative EDX analysis for the CNF_ TiO_2 sample confirming the presence of titanium dioxide. NTA analysis showed particle size distribution of PCNF and CNF_ TiO_2 samples centred at around 260 nm and 160 nm respectively for the hydrodynamic size, involving also water in primary hydration layers (Fig.1). The larger hydrodynamic size for pure cellulose nanofibers in comparison with those in CNF_ TiO_2 sample is connected with their aggregation via strong hydrogen bonding, which is apparently decreased after their coating by titania. High resolution AFM images of PCNF and CNF_ TiO_2 samples are presented in Fig.2. The obtained results also confirmed that pure cellulose nanofibers had homogeneous topography (Fig.2a).

CNF_TiO₂ sample was uniformly coated by titania nanoparticle with a size of around 10 nm (Fig.2 (b,c)). Thus, the use of CaptiGel nanosol allows to deposit uniform single layer of TiO₂-coalesced nanoparticles onto the surface of cellulose nanofibers.

According to the XRD analysis of PCNF and CNF_TiO₂ (Fig.3) the starting cellulosic material displayed a typical X-ray diffraction pattern of native cellulose-I with characteristic stronger diffraction peaks at $2\theta = 7,1^\circ$ and $10,4^\circ$ and a weaker peak as a shoulder at $2\theta = 9,3^\circ$ which refers to cellulose-II apparently present in this case. This is evidenced by the presence of clear diffraction peaks at $2\theta = 5,7^\circ(101)$ and $2\theta = 9,3^\circ(10\bar{1})$, see Tab.2. The absence of the TiO₂ diffraction peaks in the sample CNF_TiO₂ should be remarked, as it shows that the size of TiO₂ nanoparticles is smaller than the coherence domain required for the X-ray reflection. Crystallinity index was also calculated to reveal the differences between the raw cotton and the synthesized materials (Tab. 2). XRD results showed an increase in the crystallinity degree of the prepared samples via the acid hydrolysis in comparison with the RC sample. For raw cotton the crystalline index was 66.9%. Acid hydrolysis for the production of nanocrystalline cellulose improved the crystallinity index to 86%. Obviously, the increase in crystallinity originates from the removing of amorphous parts from cellulose composition during the acid hydrolysis. It is also associated with cellulose recrystallization, which results in its conversion to highly ordered state due to redistribution of the hydrogen bonds.

An insight into interaction of BTCA with titania nanoparticles on the surface of cellulose nanofibers is provided by the FTIR spectroscopy (see Fig.4). The main absorption bands for PCNF and CNF_TiO₂ samples are presented in Table TS1 (please, see supplementary). On a qualitative level, the obtained IR-spectra are quite similar, the majority of absorption peaks practically coincide. It indicates a “soft” modification process wherein the supramolecular structure of nanocrystalline cellulose remains unchanged. The broad band at 3600-3000 cm⁻¹ is observed in all synthesized samples and refers to the stretching vibrations of the hydroxyl groups involved in intermolecular hydrogen bonds.

The stretching vibrations of the CH- and CH₂-bonds of methylene and methine cellulose groups are in 2980-2830 cm⁻¹ region. The absorption peak at 1642 cm⁻¹ indicates water presence. The absorption peak at 1159 cm⁻¹ is attributed to C–O–C asymmetric stretching vibrations. However, several characteristic absorption bands show differences in the chemical structure of the obtained samples. We confirmed earlier that TiO₂ nanoparticles are cross-linked to the surface of a cotton fiber by formation of transverse ester bonds with the cross-linking agent 1,2,3,4 – butanetetracarboxylic acid (see Scheme 1).²⁹ So, the absorption peaks are assigned to carboxylic groups in CNF_TiO₂ sample after TiO₂ modification with the usage of the cross-linking agent BTCA in the 1800–1600 cm⁻¹ region. The carbonyl adsorption peak at 1710 cm⁻¹ is attributed to C=O stretching and confirmed the formation of ester bonds in the CNF_TiO₂ sample. The weak absorption peaks at 835 cm⁻¹ and 815 cm⁻¹ are attributed to Ti-O-Ti vibration (Fig.4b). The absorption band at 1420 cm⁻¹ characterizes the crystallinity, whereas the absorption band at 894 cm⁻¹ indicates the amorphous component of the samples. Thus, as a result of chemical modification of the synthesized nanocrystalline cellulose by TiO₂ nanoparticles, a decrease of the amorphous band is observed at 894 cm⁻¹, which confirms the increase in crystallinity degree in the CNF_TiO₂ sample.

Thermal stability and thermal decomposition for the raw cotton, PCNF and CNF_TiO₂ samples were investigated by thermogravimetric analysis and presented in Fig. FS1 (please, see supplementary). All samples showed a three-step weight loss. Firstly, raw cotton and PCNF together with CNF_TiO₂ samples had a small weight loss at low temperature range (less than 230°C), corresponding to the evaporation of adsorbed water. The main mass loss stage of RC, PCNF and CNF_TiO₂ samples ranged from 276°C to 360°C, with maximum thermal degradation temperature at 360°C, 348°C and 337°C, respectively. In case of cellulose nanofibers modified with TiO₂, the reason of the shift to low temperature of 337°C can be assigned to the removal of residual organics from titania. As it can be seen in Fig. FS1, the thermal stability of pure cellulose nanofibers with and without TiO₂ was higher than that of the raw cotton. It can be attributed to removal of hemicelluloses and lignin using acid hydrolysis route. Moreover, thermal stability and heat resistance also have a close relationship with the crystallinity degree. In particular, crystalline regions in cellulose are much more stable than amorphous parts in cellulose³⁴⁻³⁶. Therefore, increase of

crystallinity degree during chemical treatment also improved the heat resistance of PCNF and CNF_TiO₂ samples.

For original cotton, the maximum thermal degradation occurred at 494°C with a maximum weight loss of 99.2%. PCNF and CNF_TiO₂ samples showed a maximum thermal degradation temperature at 550°C and 548°C, respectively. In comparison to PCNF sample, the maximum weight loss of CNF_TiO₂ samples decreases by addition of titania nanoparticles and the total amount of TiO₂ is 10wt% in the obtained nanocomposites

II. Preparation and characterization of nanocomposite TiO₂-nanocellulose loaded with different drugs

Three different medicines, Diclofenac sodium, Penicillamine-D and Phosphomycin, were chosen as model drugs for modification of cellulose nanofibers and further investigation of resulting drug release system. These drugs can easily be quantified in complex systems using different methods, including spectrophotometry³⁷, chromatography³⁸ and SEM analysis. Diclofenac sodium is a potent non-steroidal compound with pronounced analgesic, anti-inflammatory and antipyretic properties. Currently, DS is used in surgery, traumatology and sports medicine, soft-tissue lesions etc. Penicillamine D (2-amino-3-mercapto-3-methylbutanoic acid) is derived from hydrolytic degradation of penicillin antibiotics and contains –SH, –NH₂ and –COOH groups. PCA-D is used as a medicinal agent against rheumatoid arthritis, and other chronic autoimmune diseases³⁹. Phosphomycin [(2R,3S-3-methyloxiran-2-yl) phosphonic acid] is a natural broad spectrum antibiotic compound which is mainly used for the treatment of uncomplicated urinary tract infections and meningitis, pneumonia, and pyelonephritis⁴⁰.

Noteworthy, different studies generally reported the use of titania nanoparticles for coating cellulose fibers for photocatalytic and antibacterial application⁴¹⁻⁴⁴. In this study, we developed a new approach using TiO₂ as active ingredient for drug delivery. The purpose of chemical modification was to synthesize a novel transdermal drug delivery system bonding a drug molecule to the biopolymer through interaction with TiO₂ grafted onto it (Scheme 2). The drug grafting was performed in amounts calculated in assumption of the formation of a uniform, single layer coverage on TiO₂-modified cellulose nanofibers' surface⁴⁶ (See supplementary material for explanation). Thus, total amounts of Diclofenac Sodium, Penicillamine D and Phosphomycin in the obtained nanocomposites were 7.7wt%, 3.8wt% and 4.7wt%, respectively. The visual optical images of the nanocomposite based on cellulose nanofibers and TiO₂ with different type of drugs such as Diclofenac Sodium, Penicillamine D and Phosphomycin, possessing high optical transparency, are presented in Fig. FS2 (please, see supplementary).

Drug modification of nanocomposite was performed by three different methods, which are described in the experimental part and named M1, M2, and M3. The first method (M1) was based on initial dissolution of drug powder in titania nanosol, followed by addition of the obtained solution to aqueous solution of the cellulose nanofibers. In the second case (M2), the drug powder was first dissolved in water and then added simultaneously with the titania nanosol to aqueous solution of the cellulose nanofibers. In the third method (M3), the titania nanosol and drug was added to aqueous suspension of the cellulose nanofibers sequentially. For instance, M1 and M2 were chosen for Diclofenac Sodium and SEM images confirmed the homogeneous distribution of drug (Fig.5(a,b)). On the contrary, M3 showed not to be suitable for DS since it agglomerates onto the cellulose nanofibers surface and does not interact with it, crystallizing as a separate phase as observed in Fig. FS3 (please, see supplementary). The availability of drugs in nanocomposite was evaluated by EDS analysis and also presented in Fig. FS3. In order to obtain uniform distribution of the drug within the cellulose nanofibers film and to bond drugs to cellulose nanofibers, the methods M1, M3 and M2, M3 were chosen for Penicillamine D and Phosphomycin, respectively. In case of using Penicillamine D, SEM images of CNF_TiO₂_PCA-D_M1 and CNF_TiO₂_PCA-D_M2 samples showed that PCA-D bonding with TiO₂ was strongly incorporated into the surface of biopolymer matrix (Fig.5(c,d)). EDX quantitative analysis for these samples confirmed the presence of titanium dioxide and

PCA-D on the samples (Fig.5(3,4)). According to SEM images of the nanocomposites modified with TiO₂ and Phosphomycin, the usage of method #2 and #3 produced a smooth and homogeneous surface with good distribution of a drug (Fig.5(e,f)).

In order to investigate possible interaction between nanocomposite and various drugs, IR- and UV-Vis spectroscopies were used. According to the obtained data from IR-spectroscopy, no new absorption peaks after drug modifications were observed for any of the synthesised nanocomposites. Absence of the characteristic peaks can be attributed to the fact that sensitivity of infrared spectroscopy does not identify such small amount of the immobilized drug. Consequently, drug molecule and nanocomposite are compatible with each other. It is important to mention that strong chemical interaction between these components may lead to complete loss of medical properties of drugs⁴⁵. At the same time, there is possibility of intermolecular interactions since the drug molecule contains various functional groups. Previously, we reported the production of a heteroligand complex between Penicillamine D as a modifying ligand and titanium alkoxide via chemisorption mechanism, involving surface chelation³². To detect the complexation of TiO₂ and the two model drugs, Diclofenac Sodium and Penicillamine D, UV-Vis spectroscopy was used. For this purpose, drug powder of DS or PCA-D was dissolved in titania nanosol. The intensity of maximum absorption peak at 224 nm was observed for pure titania nanoparticles and used as a reference³². The spectrum of the resulting solution from reaction between titania nanosol and Diclofenac sodium shows an absorption peak at 375 nm (Fig.6a). In the case of Penicillamine D, the absorption peak was centered at 474 nm (Fig.6b). These results confirmed the complexation of drugs on the surface of titania. Thus, titania binds to cellulose nanofibers via formation of ester bonds and with drug molecules due to formation of chelating complexes. The modification by different types of drugs resulted in changes to the crystalline properties of the nanocomposites. Fig.7 shows the typical X-ray diffractograms of cellulose type II with characteristics peaks at $2\theta = 5.5^\circ$ and 9.4° . The results in Table II clearly demonstrate an increase in the crystallinity degree of more than 10% after modification of drugs in comparison with pure cellulose nanofibers.

Radio-labeling analysis of ³³P-ATP interaction

The goal of this work was to develop nanocomposites as drug delivery system namely as a transdermal patches for skin application. To study the *in vitro* kinetics of Phosphomycin release from nanocomposite based on cellulose nanofibers and TiO₂, we performed radio-labeling analysis using phosphorylated drug ³³P-marked ATP as a model of Phosphomycin. Technique and examples of possible applications of this method can be found in the literature⁴⁶⁻⁴⁸. As it can be seen from Fig.8(a), no uptake is observed for the CNF sample. The uptake and release of ³³P-marked ATP from CNF_TiO₂ sample in comparison with the pure cellulose nanofibers are presented in Fig.8b. Two different concentrations of ³³P-marked ATP, 1 nM and 3 nM were measured. Firstly, 3 ml of Milli-Q-pore water with 0.1 % Tween 20 was added with 40 min measurement of baseline to the dish with CNF and CNF_TiO₂ samples. Then, 1 μl of 1 nM ³³P-marked ATP was added with 23 h of association measurement. After that, another 2 μl of ³³P-ATP was added, resulting in 3 nM ³³P-ATP in the dish with the samples for further association measurement for 21.5 h. Finally, the liquid was replaced with 3 ml of phosphate-buffered saline (PBS) and 0,1 % Tween 20 for release measurement. Previously, we reported studies of immobilization and release of ³³P-marked ATP from mesoporous titania microparticles³¹. The obtained data demonstrate great affinity of material to phosphorylated ligands with a slow release of 20% of ³³P-ATP in 200 h from these titania microparticles, which allows the application of titania microparticles as smart drug release sources. In this work, we used titania nanoparticles for cellulose nanofibers modification. Strong binding of ³³P- marked ATP with the surface of CNF_TiO₂ sample was also observed, as in pure titania microparticles³¹ (Fig.8b). In particular, ³³P-marked ATP 1nM associated and reached the equilibrium with the sample in 10 h and in more than 21.5 h for 3nM ³³P-ATP. It should be mentioned that surface saturation was not achieved with high concentration. The release of ³³P-marked ATP from CNF_TiO₂ sample occurred in two steps: firstly, 40%

of ^{33}P -marked ATP dissociated after first 4 h and only an additional 25% dissociated in the following 100 h. Thus, the synthesized nanocomposites based on cellulose nanofibers and TiO_2 are very promising material for drug delivery application possessing very slow releasing properties.

***In vitro* drug release**

According to earlier reports in literature, the release of various drug molecules from nanocrystalline cellulose and derived composites was quite rapid⁴⁹⁻⁵¹. In this work, two different methods of drug modification were used to show that various interactions between TiO_2 and drug molecule could be used to control the kinetic of long-term drug release. Firstly, to determine the TiO_2 stability in nanocomposites, we investigated *in vitro* release of titania from CNF_ TiO_2 sample. As it can be seen from the Fig. FS4, only negligible amount of titania was released from nanocomposites in 3 days. One possible reason for low release of TiO_2 may be the strong bonding between titania nanoparticles and cellulose nanofibers achieved via grafting. Fig.9 shows the release curves of Diclofenac Sodium and Penicillamine D from the nanocomposites obtained by method #1 and #2. The release mechanisms for each drugs incorporated into nanocomposite by two different methods are mostly similar and the release curve can be considered as an isotherm with saturation. Comparison between release profiles of both drugs from nanocomposite showed that DS is released much faster than PCA-D regardless of the modification method. According to obtained results, for CNF_ TiO_2 _DS_M1 sample, the release of DS is carried out with a constant speed for more than 10 hours, reaching the equilibrium in 16 hours with a total amount of DS released around 50% (Fig.9a). A similar behaviour of slow DS release was observed for CNF_ TiO_2 _DS_M2 sample, but only 28% of DS was released over 15 h (Fig.9b). The nanocomposites with Penicillamine D obtained by method #1 and #2 released the drug more slowly. The *in vitro* release profiles of PCA-D from CNF_ TiO_2 _PCA-D_M1 and CNF_ TiO_2 _PCA-D_M2 samples are shown in Fig.9(c,d). As can be seen from Fig.9(c), CNF_ TiO_2 _PCA-D_M1 sample displayed a sustained long-term release profile of Penicillamine D where around 31% of drug released in a controlled manner over 96 hours. Method #2 for incorporation of PCA-D into the nanocomposite allows reduction of the release time to 43 hours with a total amount of ~40% (Fig.9d).

Thus, these studies clearly demonstrate that using different methods of binding drug molecule to the biopolymer through interaction with TiO_2 provide slow release, and most importantly, the level of released drug remains constant over a long time. The observed difference between release times of DS and PCA-D can be also explained by different solubility of drugs in water^{52,53}. Specifically, the solubility of Diclofenac sodium⁵⁴ at 25 °C is 50 mg/ml, which is higher than that of Penicillamine D (30 mg/ml). So, swollen nanocomposites contain a large amount of water and diffusion process of a drug can proceed faster and easier than in case with PCA-D. It is important to note that using cross-linking agent for binding TiO_2 with cellulose nanofibers has important implications for the release process. In particular, burst drug release profile was observed for nanocomposite based on cellulose nanofibers and TiO_2 with DS prepared by method #1 and #2 without usage of cross-linking agent (Fig.10). The obtained results showed that 93% and 81% of the entrapped DS was completely released within 10 min from nanocomposite with DS obtained by method #1 and #2 without using BTCA to cross-link titania with cellulose nanofibers, respectively. Similar results have been reported by N. Silva et al⁵⁵. They investigated the potential application of bacterial cellulose membranes as a transdermal delivery system for the delivery of Diclofenac. In fact, about 90% of the total drug was released after 10 min. Apparently, the drug was lost together with the non-grafted titania simply washed from the material to which in the absence of the cross-linking agent it was not chemically bound. So, it can clearly be observed that application of cross-linking agent is not superfluous but necessary because the cellulose nanofibers modified only with titania and drug lose their drug delivery properties.

In perfect agreement with the main goal of this study, the nanocomposites based on cellulose nanofibers and TiO_2 modifying with three types of drug were successfully produced for dermal application with a completely controlled drug release. Depending on required therapeutic effect and period of healing, different type of nanocomposites with immobilized drug can be applied to treat diseases. In case of

Diclofenac Sodium, relatively rapid onset of analgesic and anti-inflammatory effects is required. On contrary, the use of anti-inflammatory agents such as Penicillamine D and antibiotics such as Phosphomycin requires long-term treatment. Thus, the obtained results of release kinetics are in a good agreement with the medicinal properties of drugs. Namely, depending on speed, drug release from nanocomposite based was in the following order: Diclofenac Sodium > Penicillamine D > Phosphomycin.

Thus, the obtained nanocomposites can give possibility to generate a new smart drug delivery patch with a whole complex of therapeutic properties. *In vitro* effects of a series of antibiotics incorporated into the produced slow release matrix has been investigated and will be reported separately in the near future.

The drug delivery matrices reported in the present work are employing nano titania as active component for the drug binding and retention. While TiO₂ is certified as both food additive (E171 in EU) and as solar protection factor in skin applications (FDA approved concentration in sunscreen formulations up to 25 wt%)⁵⁶ and is often used as negative control in the toxicity studies for nanoparticle materials,⁵⁷ there are still some concerns about its potential health effects.⁵⁸ The impact of nano titania on human health is strongly dependent on the size and crystallinity of the particles and the way of exposure, the introduction into the lungs through aspiration being regarded as most hazardous. The composite material in the present study is containing titania strongly bound to the matrix, so the loss into air should be considered as negligible. In the form of small nanoparticles, the titania is known to be highly bio-digestible,⁵⁹ transforming in biological fluids (containing normally appreciable concentrations of chelating carboxylate ligands such as citrate and lactate) into soluble and non-toxic carboxylato-titanate species.^{31,32,59}

Conclusions

In this work, we successfully synthesized a new type of nanocomposites based on cellulose nanofibers and modifying TiO₂ with three types of medicines, namely, Diclofenac sodium, Penicillamine-D and Phosphomycin. Experiments confirmed that drugs are uniformly distributed within the cellulose nanofiber film. One of the most important advantages of this work is the use of titania as a binding agent between cellulose nanofibers and a drug molecule, which provides a slow and controlled release. The drug release studies showed long-term release profiles with different kinetics of release depending on the medicine used. The quickest release was observed for the more soluble painkiller, slower one for the anti-inflammatory agent and the longest release took place for the strongly chemisorbed antibiotic agent. Thus, the nanocomposites produced by this technology can potentially be applied to transdermal drug delivery patches, as anesthetics, analgesics and wound-dressing materials.

Acknowledgements

The authors would like to express their gratitude to the Swedish Research Council (Vetenskapsrådet) for the support of the project "Molecular precursors and molecular models of nanoporous materials". O. Galkina would like to thank the Swedish Institute for a PhD scholarship. The authors are indebted to Bruker Nano company, and in particular to Dr. Fabrice Magne and Dr Alexandr Dulebo for the aid with AFM measurements. Dr Hanna Björkelund and Dr Karl Andersson at Ridgeview Instruments AB are gratefully acknowledged for the help with radioisotope measurements.

References

- 1 A.Y. Denisov, E. Kloser, D.G. Gray, A.K. Mittermaier, *J. Biomol. NMR*, 2010, **47**, 195.
- 2 M. Ioelovich, O. Figovsky, *Adv. Mat.Res.*, 2008, **47-50**, 1286.
- 3 C. Zhou, Q. Shi, W. Guo, L. Terrell, A. T. Qureshi, D. J. Hayes, Q. Wu, *ACS Appl. Mater. Interfaces*, 2013, **5**, 3847.

- 4 C. Vinatier, O. Gauthier, A. Fatimi, C. Merceron, M. Masson, A. Moreau, F. Moreau, B. Fellah, P. Weiss, J. Guicheux, *Biotechnol. Bioeng.*, 2009, **102**, 1259.
- 5 S. Saska, H.S. Barud, A.M.M. Gaspar, R. Marchetto, S.J.L. Ribeiro, Y. Messaddeq, *Int. J. Biomat.*, 2011, DOI:10.1155/2011/175362
- 6 A. Sannino, S. Pappada, L. Giotta, L. Valli, A. Maffezzoli, *J. Appl. Polym. Sci.*, 2007, **106**, 3040.
- 7 P. Schexnaider, G. Schmidt, *Colloid Polym. Sci.*, 2009, **287**, 1.
- 8 P. Chitprasert, P. Sudsai, A. Rodklongtan, *Carbohydr. Polym.*, **90**, 78.
- 9 B. Mukherjee, B. Mahanti, P. Panda, S. Mahapatra, *Am. J. Ther.*, 2005, **12**, 417.
- 10 C.S. Ha, J.A. Gardella, *Chem. Rev.* 2005, **105**, 4205.
- 11 A.K. Bajpai, S.K. Shukla, S. Bhanu, S. Kankane, *Prog. Polym. Sci.*, 2008, **33**, 1088.
- 12 C. Chang, B. Duan, J. Cai, L. Zhang, *Eur. Polym. J.*, 2010, **46**, 92.
- 13 S.M. Liang, L.N. Zhang, Y.F. Li, J. Xu, *Macromol. Chem. Phys.*, 2007, **208**, 594.
- 14 A. Sannino, M. Madaghiale, *Biomacromol.*, **2004**, 5, 92.
- 15 B. Fang, Y.Z. Wan, T. T. Tang, C. Gao, K. R. Dai, *Tissue Eng. Pt. A.*, 2009, **15**, 1091.
- 16 S.J. Eichhorn, A. Dufresne, A. Aranguren, *J. Mat. Sci.*, 2010, **45**, 1.
- 17 K. Oksman, A.P. Mathew, D. Bondeson, I. Kvien, *Compos. Sci. Technol.*, 2006, **66**, 2776.
- 18 X.M. Dong, J.F. Revol, D.G. Gray, *Cellulose*, 1998, **5**, 19.
- 19 R. Kolakovic, L. Peltonen, A. Laukkanen, J. Hirvonen, T. Laaksonen, *Eur. J. Pharm. Biopharm.*, 2012, **82**, 308.
- 20 S.P. Akhlaghi, R.C. Berry, K.C. Tam, *Cellulose* 2013, **20**, 1747.
- 21 J.P. Mesquita, C.L. Donnici, F.V. Pereira, *Biomacromol.*, 2010, **11**, 473.
- 22 J.K. Jackson, K. Letchford, B.Z. Wasserman, L. Ye, W.Y. Hamad, H. M. Burt, *Int J. Nanomedicine*, 2011, **6**, 321.
- 23 A. Azad, A. Aboelzahab, V. Goel, *Adv. Materials. Res.*, 2012, **1**, 309.
- 24 M. Vallet-Regi, F. Balas, M. Colilla, M. Manzano, *Solid State Sci.*, 2007, **9**, 768.
- 25 A.A. Ayon, M. Cantu, K. Chava, C.M. Agrawal, M.D. Feldman, D. Johnson, D. Patel, D. Marton, E. Shi, *Biomed. Mater.*, 2006, **1**, L11.
- 26 M.S. Aw, K. Gulati, D. Losic, *J. Biomater. Nanobiotechnol.*, 2011, **2**, 477.
- 27 H. Li, T.Y. Ma, D.M. Kong, Z.Y. Yuan, *Analyst*, 2013, **138**, 1084.
- 28 O.L. Galkina, V.V. Vinogradov, A.V. Vinogradov, A.V. Agafonov, *Nanotechnologies in Russia*, 2012, **7**, 604.
- 29 O.L. Galkina, A. Sycheva, A. Blagodatskiy, G. Kaptay, V.L. Katanaev, G.A. Seisenbaeva, V.G. Kessler, A.V. Agafonov, *Surf. Coat. Tech.*, 2014, **253**, 171.
- 30 H. Björke, K. Andersson, *Appl. Radiat. Isot.*, 2006, **64**, 901
- 31 G.A. Seisenbaeva, M.P. Moloney, R. Tekoriute, A. Hardy-Dessources, J.M. Nedelec, Y.K. Gun'ko, V.G. Kessler, *Langmuir* 2010, **26**, 9809.
- 32 V.G. Kessler, G.A. Seisenbaeva, M. Unell, S. Håkansson, *Angew Chem Int Ed Engl.*, 2008, **47**, 8506.
- 33 M.I. Walsh, A. M. El. Brashy, M. E. S Metwally, A. A Abdelal, *IL FARMACO*, 2004, **59**, 493.
- 34 H. Kawamoto, W. Hatanaka, S. Saka, *J. Anal. Appl. Pyrolysis*, 2006, **76**, 280.
- 35 A. Basch, M. Lewin, *J. Polym. Sci., Part A: Polym. Chem.*, 1973, **11**, 3071.
- 36 A. Broido, A. C. Javier-Son, A. C. Ouano, E. M. Barrall, II, *J. Appl. Polym. Sci.*, 1989, **37**, 3627.
- 37 G.G. Pargaonkar, S.G. Kashedikar, *Indian Drugs*, 1994, **31**, 590.
- 38 G.S. Devika, M. Sudhakas and J.V. Rao, *Orient. J. Chem.*, 2012, **28**, 887.
- 39 A. Członkowska, J. Gajda, M. Rodo, *J. Neurol.*, 1996, **243**, 269.
- 40 A. Castañeda-García, J. Blázquez, A. Rodríguez-Rojas, *Antibiotics* 2013, **2**, 217.
- 41 J. Wang, W. Liu, *Chem. Eng. J.*, 2013, **228**, 272.
- 42 Y. Lu, Q. Sun, T. Liu, D. Yang, Y. Liu, J. Li, *J. Alloys Compd.*, 2013, **577**, 569.
- 43 C. Schütz, J. Sort, Z. Bacsik, V. Oliynyk, E. Pellicer, A. Fall, L. Wågberg, L. Berglund, L. Bergström, G. Salazar-Alvarez, *PLoS One*. 2012, **7**, DOI: 10.1371/journal.pone.0045828
- 44 M. Kemell, V. Pore, M. Ritala, M. Leskelä, M. Lindén, *J. Am. Chem. Soc.*, 2005, **127**, 14178.
- 45 N.D. Burkhanova, S.M. Yugai, S.S. Khalikov, M.M. Turganov, G.V. Nikonovich, Kh.N. Aripov, *Chem. Nat. Compd.*, 1997, **33**, 340.
- 46 R. Pazik, R. Andersson, L. Kepinski, J.M. Nedelec, V. G. Kessler, G. A. Seisenbaeva, *J. Phys. Chem. C*, 2011, **115**, 9850.
- 47 H. Björke, K. Andersson, *Appl. Radiat. Isot.*, 2006, **64**, 32.
- 48 M. Nestor, K. Andersson, H. Lundqvist, *J. Mol. Recogn.*, 2008, **21**, 179.
- 49 J.K. Jackson, K. Letchford, B. Z. Wasserman, L. Ye, W.Y. Hamad, H. M. Burt, *Int. J. Nanomedicine*, 2011, **6**, 321

- 50 S.P. Akhlaghi, D.Tiong, R.M. Berry, K.C. Tam, *Eur. J. Pharm. Biopharm.*, 2014, **88**, 207
- 51 H.M. Fahmy, M.M.G. Fouda, *Carbohydr. Polym.*, 2008, **73**, 606.
- 52 E. Castro, V. Mosquera, I. Katime, *Nanomater. Nanotechnol.*, 2012, **2**, DOI: 10.5772/50338
- 53 R. Kolakovic, T. Laaksonen, L. Peltonen, A. Laukkanen, J. Hirvonen, *Int. J. Pharmaceutics*, 2012, **430**, 47
- 54 A. Llinàs, J. C. Burley, K. J. Box, R.C. Glen, J. M. Goodman, *J. Med. Chem.*, **2007**, 50, 979.
- 55 N. Silva, A. Rodrigues, I. F. Almeida, P. C. Costa, C. Rosado, C. P. Neto, A. Silvestre, C. Freire, *Carbohydr. Polym.*, 2014, **106**, 264.
- 56 <http://www.fda.gov/ForConsumers/ConsumerUpdates/ucm258416.htm>
- 57 H. Karlsson, A.R. Gliga, F.M.G.R. Calleja, C.S.A.G. Goncalves, I. Odnevall Wallinder, H. Vrieling, B. Fadeel, G. Hendriks, *Particle Fibre Toxicol.*, 2014, **11**, 41.
- 58 a) X.H. Chang, Y. Zhang, M. Tang, B. Wang, *Nanoscale Res. Lett.*, 2013, **8**, 51; b) F.M. Christensen, H.J. Johnston, V. Stone, R.J. Aitken, S. Hankin, S. Peters, K. Ashberger, *Nanotoxicol.*, 2011, 5, 110.
- 59 a) Y.L. Cai, M. Strömme, K. Welch, *Plos One*, 2013, **8**, e75929; b) N. Groenke, G.A. Seisenbaeva, V. Kaminsky, B. Kost, V.G. Kessler, *RSC Adv.*, 2012, **2**, 4228; c) G.A. Seisenbaeva, G. Daniel, J.M. Nedelec, V.G. Kessler, *Nanoscale*, 2013, **5**, 3330.

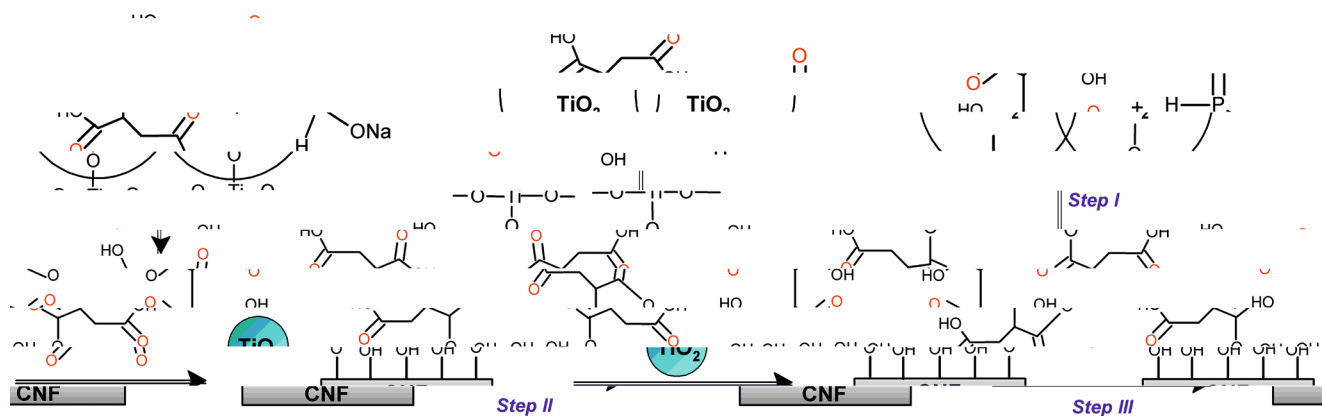
Table 1 Composition of the samples

Sample	BTCA (mol)	SHP (mol)	TiO ₂ (mol)	Drug (mol)	Method of modification
CNF_TiO ₂	0,002	0,002	1,5·10 ⁻⁴	-	-
CNF_TiO ₂ _DS_M1	0,002	0,002	1,5·10 ⁻⁴	4,74·10 ⁻⁵	Method #1
CNF_TiO ₂ _DS_M2	0,002	0,002	1,5·10 ⁻⁴	4,74·10 ⁻⁵	Method #2
CNF_TiO ₂ _PCA-D_M1	0,002	0,002	1,5·10 ⁻⁴	4,74·10 ⁻⁵	Method #1
CNF_TiO ₂ _PCA-D_M2	0,002	0,002	1,5·10 ⁻⁴	4,74·10 ⁻⁵	Method #2
CNF_TiO ₂ _Phos_M2	0,002	0,002	1,5·10 ⁻⁴	4,74·10 ⁻⁵	Method #2
CNF_TiO ₂ _Phos_M3	0,002	0,002	1,5·10 ⁻⁴	4,74·10 ⁻⁵	Method #3

Table 2 X-ray diffraction results

Sample	Peak position (2θ)				Crystalline index (CrI, %)
	(101)	(110)	(10 $\bar{1}$)	200	
	Cell-II	Cell-I	Cell-II	Cell-I	
RC	-	7.1	9.3	10.4	66.9
PCNF	5.7	-	9.3	-	86.2
CNF_TiO ₂	5.8	-	9.2	10.4	86.2
CNF_TiO ₂ _DS_M1	5.7	-	9.2	-	97.9
CNF_TiO ₂ _DS_M2	5.5	-	9.3	-	98.1
CNF_TiO ₂ _PCA-D_M1	5.5	-	9.3	-	97.0
CNF_TiO ₂ _PCA-D_M2	5.5	-	9.2	-	97.3
CNF_TiO ₂ _Phos_M2	5.6	-	9.3	-	96.0
CNF_TiO ₂ _Phos_M3	5.4	-	9.4	-	95.7

Scheme 1 Proposed mechanism of interaction of pure cellulose nanofibers with BTCA and TiO₂



Scheme 2 Proposed scheme for the interaction of nanocomposite based on cellulose nanofibers and TiO₂ with different types of drugs

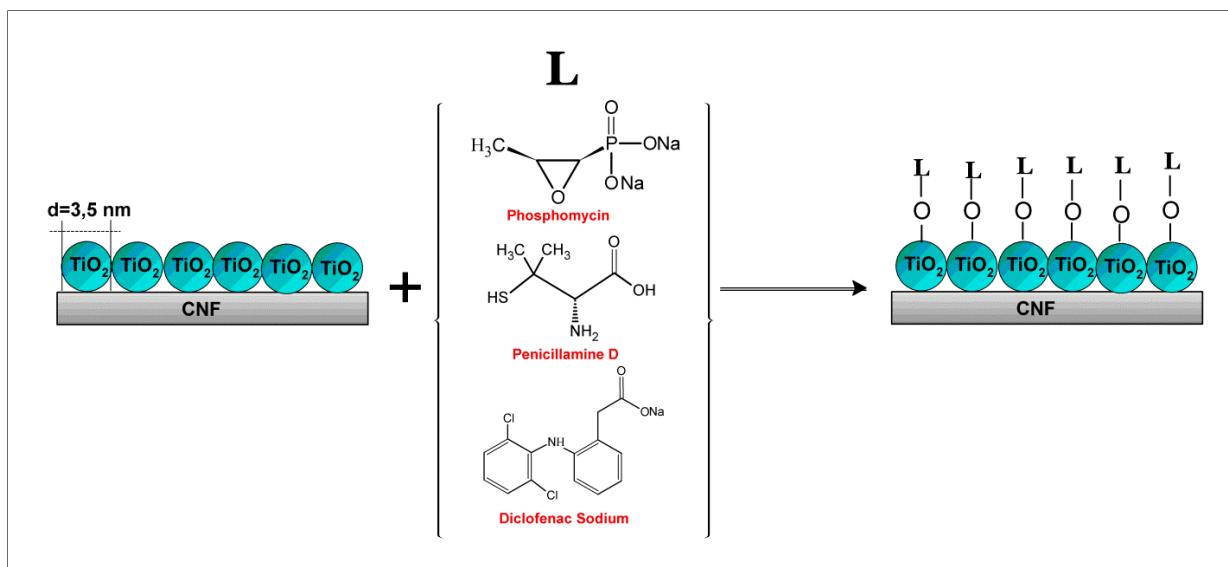


Figure.1 SEM and TEM images of (a,b) PCNF and (c,d) CNF_TiO₂ respectively together with the hydrodynamic size of pure cellulose nanofibers and nanocomposite based on cellulose nanofibers modified with TiO₂

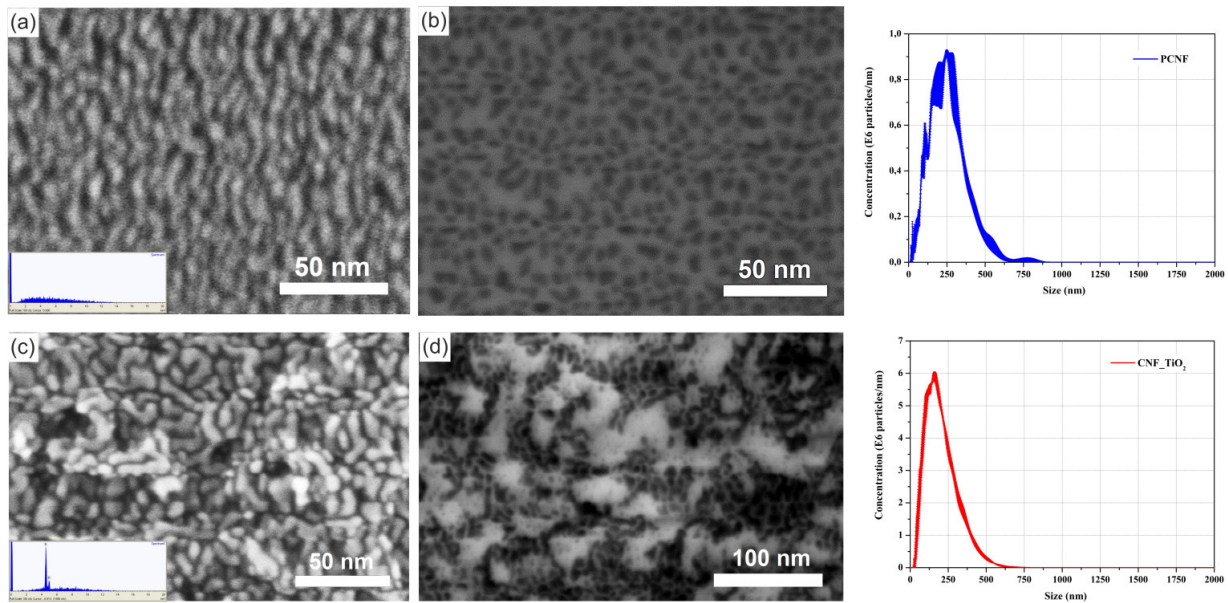


Figure.2 AFM images of (a) PCNF and CNF_TiO₂ samples (b,c)

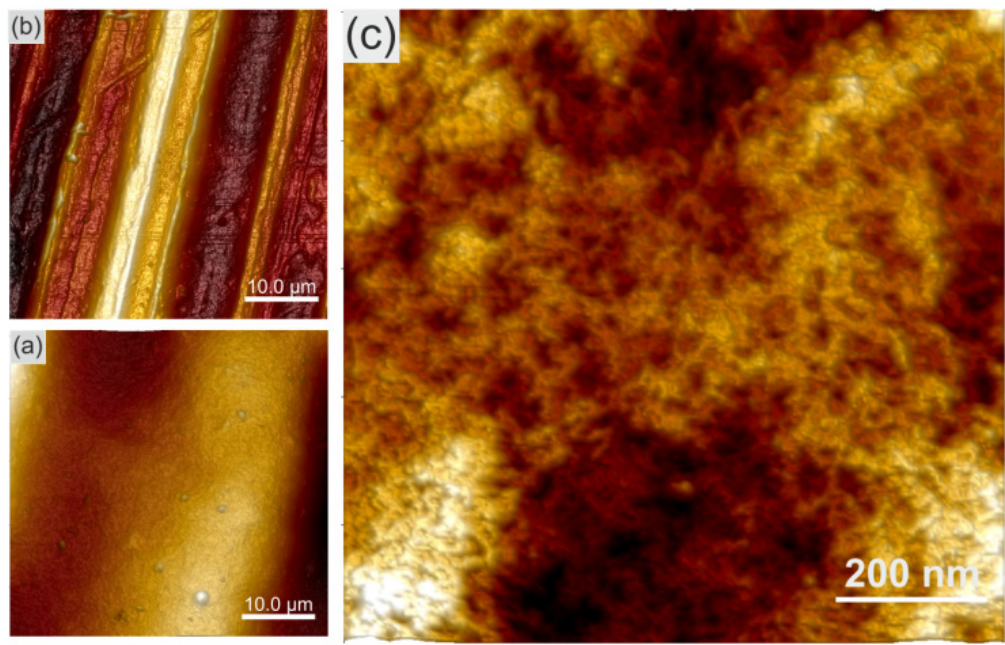


Figure.3 X-ray diffraction patterns of (a) RC; (b) PCNF and (c) CNF_TiO₂

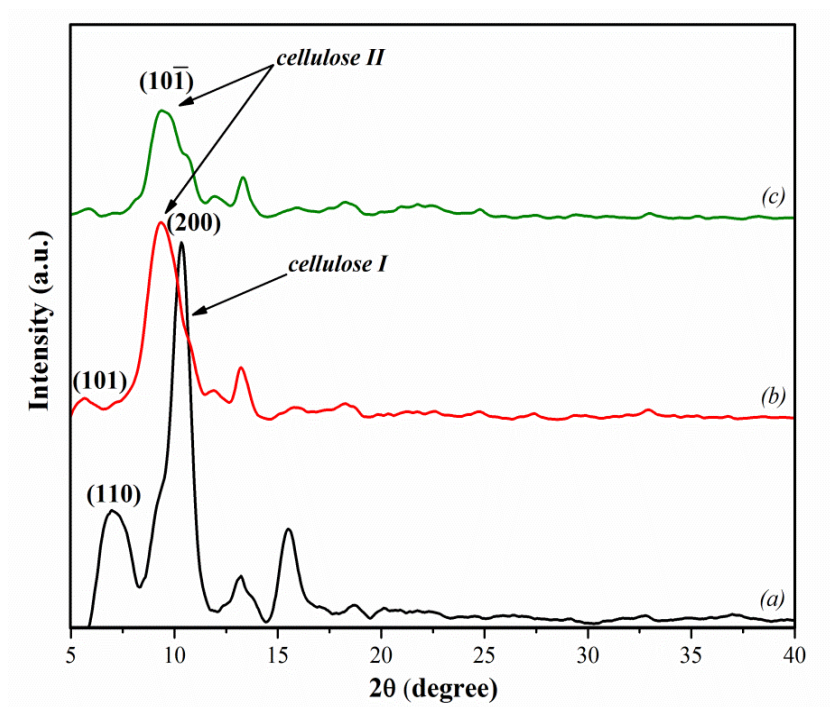


Figure.4 FTIR spectra of (a) PCNF and (b) CNF_TiO₂

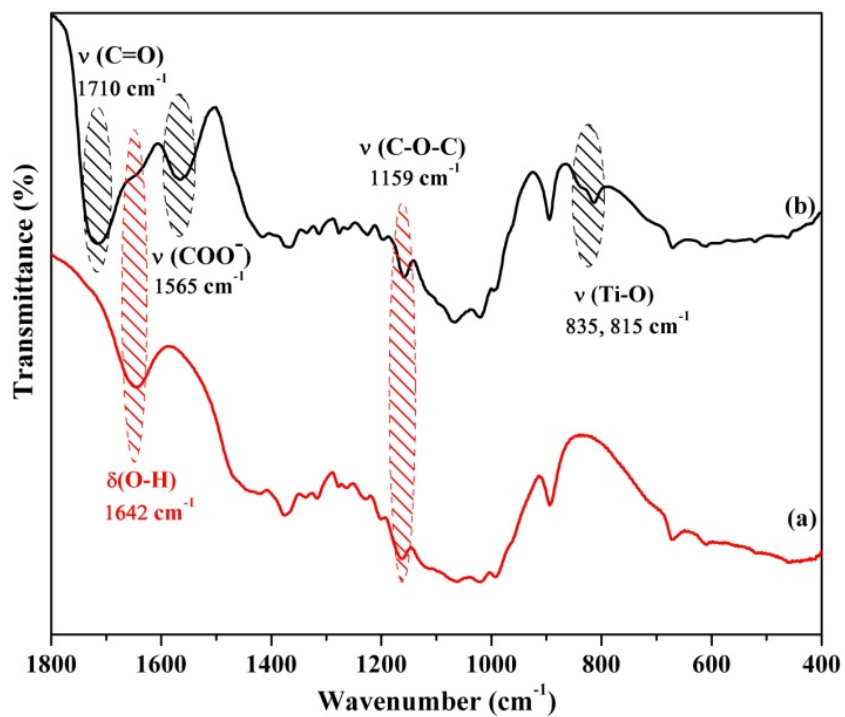


Figure.5 SEM micrographs and EDX analysis of the samples: (a,1) CNF_TiO₂_DS_M1, (b,2) CNF_TiO₂_DS_M2, (c,3) CNF_TiO₂_PCA-D_M1, (d,4) CNF_TiO₂_PCA-D_M2, (e,5) CNF_TiO₂_Phos_M2, (f,6) CNF_TiO₂_Phos_M3

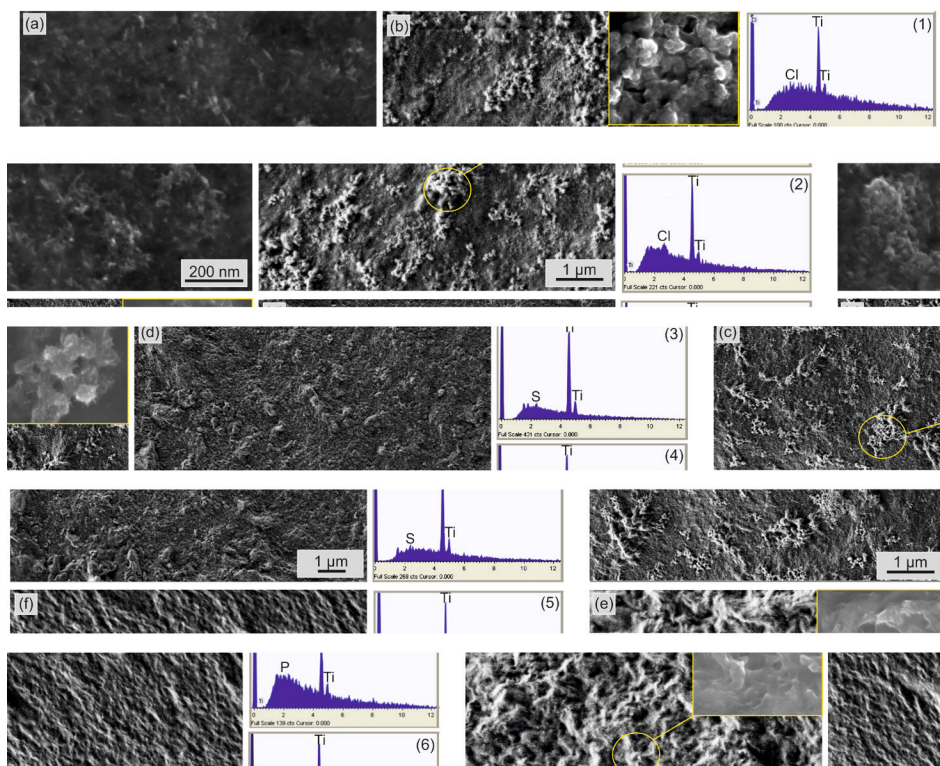


Figure.6 UV spectrum of the resulting solution from reaction between titania and Diclofenac sodium (a); between titania and Penicillamine D (b)

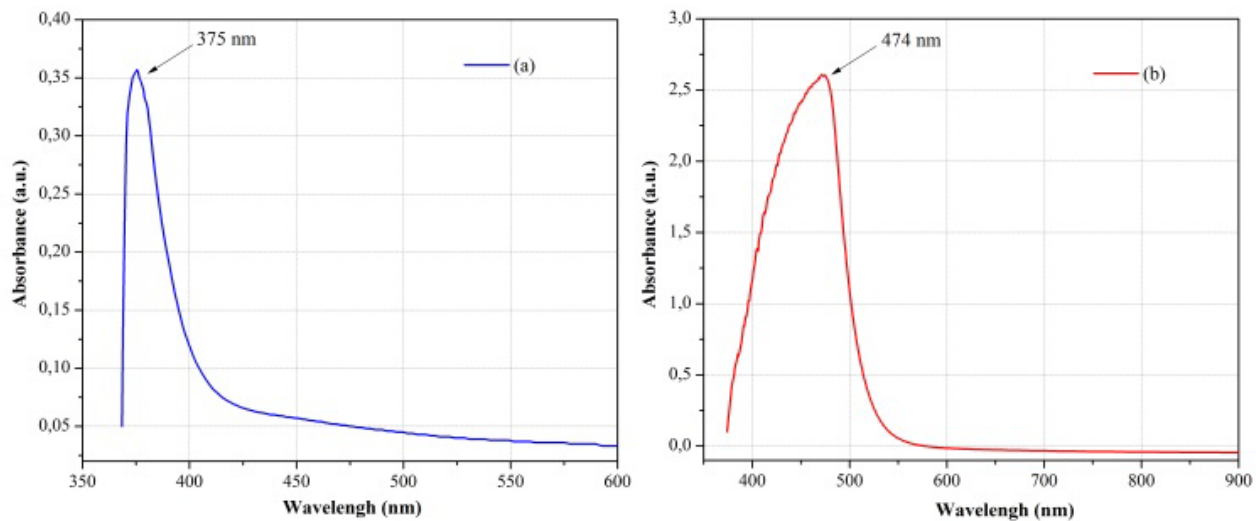


Figure.7 X-ray diffraction of the nanocomposites based on cellulose nanofibers modifying with TiO₂ and different drugs

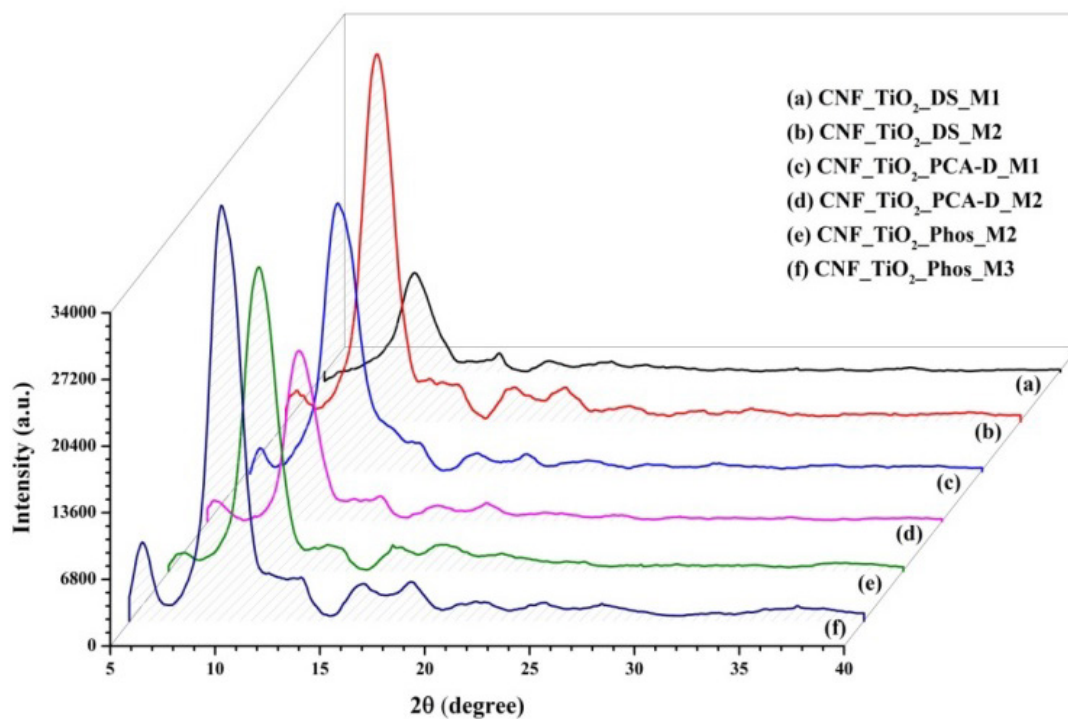


Figure.8 Real-time binding and release curve of 1 nM and 3 nM ³³P-marked ATP to (a) CNF and (b) CNF_TiO₂ sample

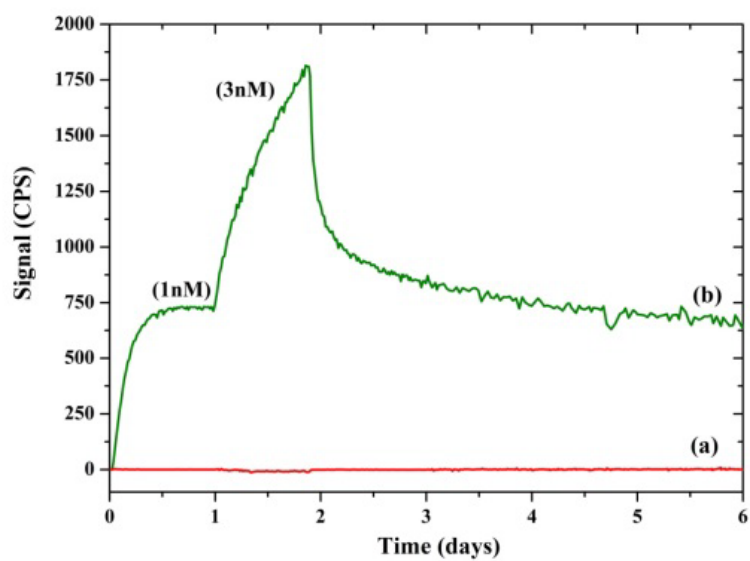


Figure.9 In vitro drug release profiles from the obtained nanocomposites: (a) CNF_TiO₂_DS_M1, (b) CNF_TiO₂_DS_M2, (c) CNF_TiO₂_PCA-D_M1, (d) CNF_TiO₂_PCA-D_M2

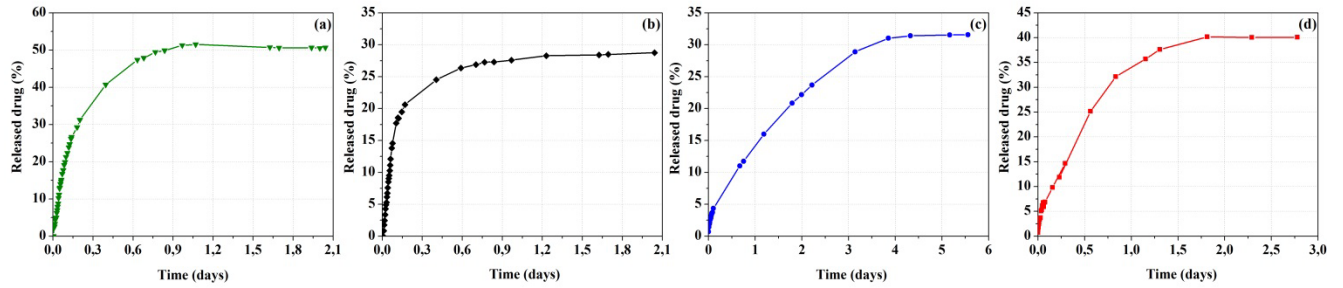


Figure.10 In vitro diclofenac sodium release profile from the nanocomposites based on cellulose nanofibers and TiO₂ with DS obtained by method #1 (b) and #2 (a) without using cross-linking agent.

